applied sciences

MDPI

Article

Mechanical and Post-Cracking Performance of Recycled and Commercial Steel Fiber-Reinforced Concrete

Cansu Colak * and Ozkan Sengul

Faculty of Civil Engineering, Istanbul Technical University, 34469 Istanbul, Türkiye
* Correspondence: colakcan@itu.edu.tr

Abstract

Recycled steel fibers (RFs) recovered from end-of-life tires (ELTs) are a potential alternative to manufactured steel fibers in concrete, but their irregular geometry may limit their effectiveness. This study compared RF and commercial hooked-end steel fibers (CFs) in ordinary Portland cement concrete produced at water-to-cement ratios (w/c) of 0.40, 0.50, and 0.60 with fiber dosages of 15, 30, and 45 kg/m^3. Workability, compressive strength, flexural strength, residual flexural strengths (f_{R1} and f_{R3}), and toughness were determined, and a multi-response desirability approach combining compressive strength, f_{R3}, and toughness was applied. Both fiber types improved the post-cracking response; however, CF provided higher residual strengths and toughness, whereas RF reduced workability more and showed a greater loss of residual capacity between f_{R1} and f_{R3}. Compressive strength was governed mainly by w/c rather than fiber dosage. The highest overall desirability was obtained with 45 kg/m^3 of CF and a w/c of 0.40, with a geometric mean (D) of 0.653, while for RF the maximum was obtained with 30 kg/m^3 and w/c = 0.40 (D = 0.285). RF effectiveness depends on matrix quality and dosage, and RF should be selected according to the required post-cracking performance rather than as a direct replacement for CF.

Keywords: recycled tire steel fiber; steel fiber-reinforced concrete; residual flexural strength; post-cracking behavior; toughness; desirability function; end-of-life tires; commercial hooked-end steel fibers

1. Introduction

End-of-life tires (ELTs) represent a substantial waste stream with significant potential for material recovery. In Europe, 95% of ELTs were collected and treated in 2019, primarily through material recycling and energy recovery [1]. Car and truck tires contain approximately 10–20% steel by mass, and the recycling of ELTs has been estimated to save 1.4–1.6 t CO_2-eq per tonne of tires compared with incineration [2]. Although steel can be recycled through remelting with almost no loss of quality [3], the direct reuse of tire-derived steel fibers in cementitious materials is particularly attractive because it can provide a secondary reinforcement source while reducing the need for newly manufactured steel. However, recycled tire steel fibers (RFs) exhibit considerable variability in length, geometry, and surface condition as a consequence of tire composition and recycling processes [4,5].

Steel fiber-reinforced concrete (SFRC) improves the inherently brittle response of cementitious materials by enhancing crack control, toughness, and post-cracking load-carrying capacity [6]. These improvements depend strongly on fiber geometry, dosage, orientation, and distribution [7,8]. Commercial steel fibers (CFs) provide controlled geometry and anchorage, whereas RFs recovered from ELTs are generally more irregular and

Check for updates

Academic Editor: Doo Yeol Yoo

Received: 12 October 2026
Revised: 29 October 2026
Accepted: 2 November 2026
Published: 5 November 2026

Copyright: © 2026 by the authors. Licensee MDPI, Basel, Switzerland. This article is an open access article distributed under the terms and conditions of the Creative Commons Attribution (CC BY) license.

may contain residual rubber or surface contamination. Consequently, although RFs can improve the mechanical response of concrete, their flexural performance at comparable dosages may remain below that of manufactured fibers [9–11]. Nevertheless, their lower material cost and potential for material recovery make them attractive as an alternative reinforcement where moderate post-cracking performance is sufficient.

Residual flexural performance is particularly important for evaluating the contribution of steel fibers after cracking. Previous studies have shown that residual strength parameters are sensitive to fiber distribution, orientation, and specimen geometry, with later-stage residual responses providing useful information on post-cracking behavior [12]. Senesavath et al. [13] compared purified and non-purified recycled tire steel fibers with industrial steel fibers at a constant fiber dosage of 30 kg/m^3 and reported that recycled fibers improved flexural response and toughness, with purified fibers providing better performance than non-purified fibers. More recent studies have also demonstrated that appropriate processing and selection of recycled tire steel fibers can substantially improve their effectiveness [14]. However, differences in matrix composition, fiber characteristics, and dosage make direct comparison among existing studies difficult.

Most investigations of RF-reinforced concrete have focused on individual fiber systems or a limited range of mixture parameters. Recent studies have examined the mechanical and durability performance of concrete containing recycled tire steel fibers [15], the incorporation of untreated RFs at a single dosage into structural concrete with electric arc furnace slag aggregates [16], and waste-derived fibers in high-performance cementitious systems [17]. Previous work has also compared the residual flexural performance of recycled and commercial steel fibers in slag-blended concrete [18]. However, comparatively limited attention has been given to the systematic comparison of RF and CF across different matrix qualities and fiber dosages in ordinary Portland cement (OPC) concrete under identical experimental conditions. In particular, the combined influence of water-to-cement ratio, fiber type, and fiber dosage on workability, compressive strength, and post-cracking flexural response remains insufficiently understood.

Accordingly, this study systematically compares RF and CF in OPC concrete produced at three water-to-cement ratios (0.40, 0.50, and 0.60) and three fiber dosages (15, 30, and 45 kg/m^3) under identical mixing, casting, and testing conditions. The effects of fiber type and dosage are evaluated in terms of workability, compressive strength, flexural strength, residual flexural strengths at early and advanced crack openings (f_{R1} and f_{R3}), and toughness, in order to clarify how the relative effectiveness of RF changes with matrix quality and fiber content. Because these responses do not necessarily improve simultaneously, a multi-response desirability approach is subsequently applied to compressive strength, f_{R3}, and toughness, using common normalization bounds for all fiber-reinforced mixtures, to identify the fiber type–dosage combinations that provide the most balanced mechanical performance for each matrix quality. Rather than treating RF as a direct substitute for CF at a single dosage, the study thereby provides a comparative framework for assessing the conditions under which recycled tire steel fibers can be used as an alternative to manufactured steel fibers in OPC concrete.

2. Materials and Methods

2.1. Materials and Mix Design

OPC (CEM I 42.5 R) was used as the binder in all mixtures. Natural sand, crushed stone sand (C. sand), and two sizes of crushed coarse aggregates (CS NoI and CS NoII) were used, with a maximum aggregate size of 31.5 mm. The aggregates were combined in constant proportions (by mass) of 0.20 natural sand, 0.30 C. sand, 0.25 CS NoI, and 0.25 CS NoII for all mixtures, and their particle size distributions are given in Table 1.

A polycarboxylate-based superplasticizer (SP) (Sika® ViscoCrete®-520 P, Sika AG, Baar, Switzerland) was used to obtain the required workability without altering the w/c.

Table 1. Particle size distribution of the aggregates and of the combined aggregate blend.

Sieve Size (mm)	Natural Sand	C. Sand	CS NoI	CS NoII	Mix
31.5	100	100	100	100	100
16	100	100	100	48	87.0
8	100	98	59	0.3	64.2
4	100	89	2.4	0.3	47.4
2	99	54	1.6	0.3	36.5
1	98	29	1.6	0.3	28.8
0.5	95	17	1.5	0.3	24.6
0.25	17	9	1.5	0.3	6.6
Mix ratio	0.20	0.30	0.25	0.25	-

Two types of steel fibers were investigated: RFs recovered from ELTs by mechanical shredding and CFs. The RFs exhibited irregular geometry and a broad distribution of length and diameter and contained residual rubber and textile fragments after recovery. Before mixing, the RFs were manually cleaned and disentangled and were gradually introduced into the mixer to minimize fiber balling. Representative images of the RFs and CFs are shown in Figure 1, and their geometrical characteristics are summarized in Table 2. The CFs were hooked-end, bright, glued steel fibers (Dramix® 3D 80/60BG, Bekaert, Zwevegem, Belgium) with a length of 60 mm, a diameter of 0.75 mm (aspect ratio of 80), a nominal tensile strength of 1225 MPa, and a Young's modulus of 200 GPa [19].



(a) (b)

Figure 1. RF and CF geometry. (**a**) RFs as recovered from end-of-life tires (**left**) and CFs (**right**) (a single fiber and a glued bundle); (**b**) RFs after manual cleaning and disentangling. The rulers are graduated in centimeters.

Table 2. Geometrical characteristics and mass fractions of RF.

RF Class	Diameter (mm)	Length (mm)	Aspect Ratio (l/d)	Mass Fraction (%)
Thin	0.31 ± 0.06	18.4 ± 7.8	59.0	12.0
Medium	0.38 ± 0.13	68.0 ± 25.0	178.8	40.8
Coarse	1.19 ± 0.65	71.3 ± 26.9	60.0	47.2

Concrete mixtures were produced at w/c of 0.40, 0.50, and 0.60. For each w/c, RF and CF were incorporated at dosages of 15, 30, and 45 kg/m^3, corresponding to fiber volume fractions of approximately 0.19%, 0.38%, and 0.57%, respectively and together with a fiber-free reference mixture. The aggregate proportions were kept constant, while the superplasticizer dosage was adjusted to achieve suitable workability. A total of 21 concrete

mixtures were investigated. The mixtures were designated according to the w/c, fiber dosage, and fiber type. For example, 0.50/30RF denotes a mixture with w/c = 0.50 containing 30 kg/m^3 of RFs, while 0.50/30CF represents the corresponding mixture containing CFs. Fiber-free mixtures were designated as 0.40/Ref, 0.50/Ref, and 0.60/Ref. The mixture proportions and slump values are given in Table 3.

Table 3. Concrete mix design and slump values.

Materials (kg/m^3)	0.40/Ref	0.50/Ref	0.60/Ref	0.40/15	0.50/15	0.60/15	0.40/30	0.50/30	0.60/30	0.40/45	0.50/45	0.60/45
Cement	350	350	350	350	350	350	350	350	350	350	350	350
Water	140	175	210	140	175	210	140	175	210	140	175	210
Sand	417	371	353	383	364	342	383	363	340	386	366	343
C. Sand	639	569	542	587	558	525	586	557	522	592	561	526
CS NoI	532	474	451	489	465	437	485	464	435	493	467	439
CS NoII	532	474	451	489	465	437	485	464	435	493	467	439
Fiber	0	0	0	15	15	15	30	30	30	45	45	45
SP for RF (%)	1.3	1	0.5	3	2	1	4	2.4	1.2	5.5	3	1.8
SP for CF (%)				2	1.5	0.5	3	2	0.5	5	3	2
Slump RF (cm)	16	20	23	11	13	16	8	10	12	1	7	9
Slump CF (cm)				19	22	19	15	18	19	14	14	16

2.2. Testing Procedure

Fresh concrete workability was evaluated using the slump test. All specimens were demolded after 24 h and cured in water at 20 ± 2 °C until testing at 28 days. Compressive strength was determined on 100 × 200 mm cylindrical specimens at 28 days in accordance with EN 12390-3 [20]. Three cylinders were tested for each mixture.

Flexural performance was evaluated by three-point bending tests on notched prismatic specimens, following the procedure of EN 14651 [21] adapted to 100 × 100 × 500 mm beams, as in a previous study [18]. A saw-cut notch with a depth of $a_0 = 17 \pm 1$ mm was made at mid-span, giving an effective ligament height of $h_{sp} = 83$ mm. The beams were tested over a clear span of 425 mm on knife-edge supports. The crack mouth opening displacement (CMOD) was measured with a clip gauge placed across the notch mouth, and the tests were run under CMOD control at a constant rate of 0.05 mm/min until a CMOD of 4.0 mm was reached, at which point the tests were terminated. All mixtures were tested with the same geometry and control settings, with three beams per mixture.

The maximum flexural strength (f_{flex}) was calculated from the maximum load recorded during the test, and the residual flexural strengths f_{R1} and f_{R3} from the loads at CMOD values of 0.5 and 2.5 mm, respectively:

$$f_{flex} = \frac{3Fl}{2bh_{sp}{}^2} \quad (1)$$

where f_{flex} is the flexural strength (MPa), F is the corresponding load (N), l is the clear span (425 mm), b is the beam width (100 mm), and h_{sp} is the effective ligament height (83 mm). Toughness was calculated as the area under the load–CMOD curve up to CMOD = 4.0 mm.

2.3. Multi-Criteria Performance Assessment

A multi-response desirability approach was used to compare the overall performance of the concrete mixtures. The desirability function method proposed by Derringer and Suich [22] transforms each response into an individual desirability value (d_i) ranging from 0 to 1, where 0 represents the least desirable and 1 the most desirable response. Compressive strength (d_1), the residual flexural strength at CMOD = 2.5 mm, f_{R3} (d_2), and toughness

(d_3) were treated as maximization criteria. A linear desirability function with a weighting factor of 1 was adopted, and the individual desirability of each response was calculated as:

$$d_i = \begin{cases} 0, & Y_i < L_i \\ \frac{Y_i - L_i}{U_i - L_i}, & L_i \le Y_i \le U_i \\ 1, & Y_i > U_i \end{cases} \quad (2)$$

where Y_i is the measured value of response i, and L_i and U_i are the lowest and highest values of that response observed among all fiber-reinforced mixtures, respectively. The individual desirability values were then combined into the overall desirability (D) using the geometric mean:

$$D = (d_1 \times d_2 \times d_3)^{1/3} \quad (3)$$

To visualize the variation in D with w/c and fiber dosage a second-order polynomial was fitted by least squares to the nine mixtures of each fiber type:

$$D = a_0 + a_1(w/c) + a_2F + a_3(w/c)F + a_4(w/c)^2 + a_5F^2 \quad (4)$$

where F is the fiber dosage (kg/m^3) and a_0–a_5 are the fitted coefficients. Because six coefficients were fitted to nine data points, the fitted surfaces were used only as graphical trend guides and not as predictive models.

Equal importance was assigned to the three responses. All 18 fiber-reinforced mixtures were evaluated together using common normalization bounds, so that the resulting D values are directly comparable across the investigated w/c ratios and fiber type–dosage combinations. Because the bounds correspond to the experimentally observed extremes, the D values express the relative mechanical performance of the mixtures within the investigated experimental domain rather than an absolute performance measure.

3. Results and Discussion

3.1. Workability and Compressive Strength

The slump results for all mixtures are presented in Table 3. Increasing the RF dosage from 15 to 45 kg/m^3 reduced the slump from 11 to 1 cm, 13 to 7 cm, and 16 to 9 cm at w/c ratios of 0.40, 0.50, and 0.60, respectively. In comparison, CF mixtures containing 45 kg/m^3 maintained slump values of 14, 14, and 16 cm, indicating a considerably greater loss of workability with RF, particularly at low w/c. Similar reductions in slump with increasing waste or recycled steel fiber content have been reported in previous studies [23–25], mainly due to increased fiber interaction and internal friction within the fresh mixture.

The 28-day compressive strength results are presented in Figure 2. The reference mixtures exhibited compressive strengths of 70.0, 50.7, and 45.2 MPa at w/c of 0.40, 0.50, and 0.60, respectively, demonstrating the dominant influence of matrix quality. At w/c = 0.40, the fiber-reinforced mixtures ranged from 60.0 to 70.8 MPa, whereas the corresponding ranges were approximately 45.8–54.8 MPa at w/c = 0.50 and 41.1–44.0 MPa at w/c = 0.60. Three-way ANOVA (w/c, fiber type, and dosage; three specimens per mixture) showed that w/c explained about 90% of the total variation in compressive strength ($p < 0.001$), whereas fiber type and dosage together explained only about 3%. Fiber addition did not increase compressive strength relative to the reference mixtures, and several mixtures showed small but significant reductions (Dunnett's test, $p < 0.05$). No systematic increase in compressive strength was observed with increasing fiber dosage. This limited influence of steel fibers on compressive strength is consistent with previous studies [26,27], which reported that fiber incorporation has a relatively minor effect on compressive strength compared with its contribution to tensile and post-cracking behavior.

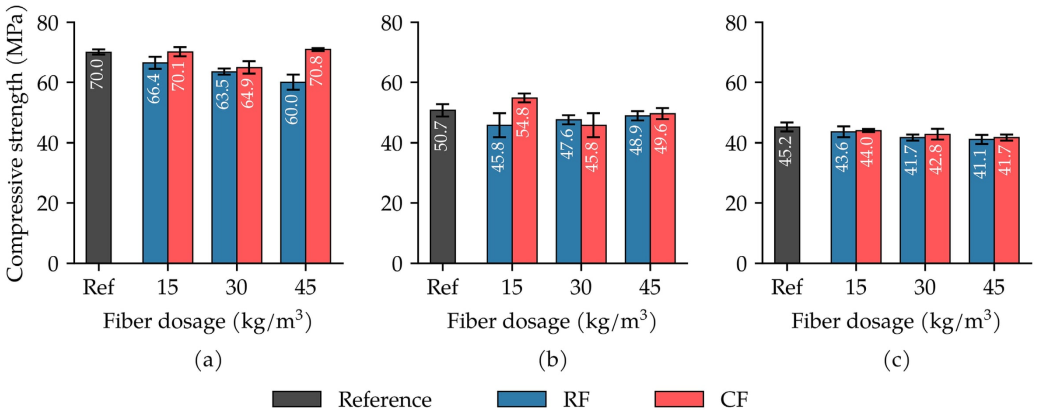


Figure 2. Compressive strength of RF- and CF-reinforced concrete at different fiber dosages ((**a**) w/c = 0.40, (**b**) w/c = 0.50, (**c**) w/c = 0.60). Error bars represent ± standard deviation.

3.2. Post-Cracking Flexural Properties

The flexural response of the mixtures was evaluated from the load–CMOD curves obtained during three-point bending tests. The representative curves (Figure 3) were selected to illustrate the characteristic post-cracking behavior without presenting all individual responses. These curves provide a direct comparison of the influence of fiber type and matrix quality on the post-cracking response.

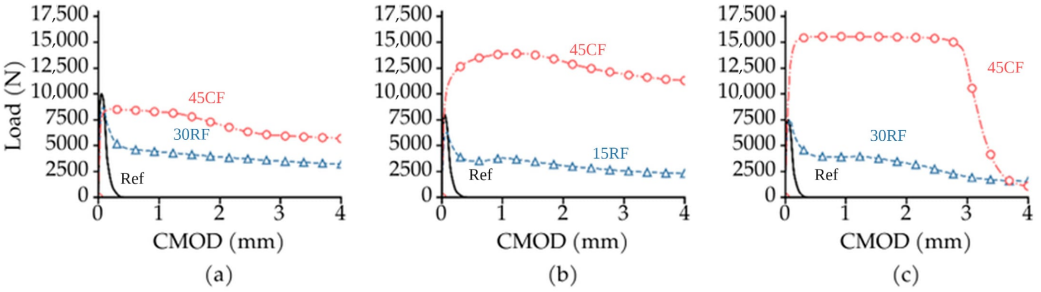


Figure 3. Representative load–CMOD curves of SFRC mixtures at different w/c ratios: (**a**) w/c = 0.40, (**b**) w/c = 0.50, and (**c**) w/c = 0.60.

The flexural strength (f_{flex}) results for all mixtures are presented in Figure 4. The reference mixtures exhibited f_{flex} values of 8.3, 7.0, and 5.5 MPa at w/c of 0.40, 0.50, and 0.60, respectively. The incorporation of fibers generally increased the maximum flexural strength, although the magnitude of the improvement depended on fiber type, dosage, and matrix quality. For RF mixtures, the highest f_{flex} values were 8.9, 8.9, and 8.4 MPa at w/c ratios of 0.40, 0.50, and 0.60, respectively. CF produced a more pronounced improvement, with maximum values of 11.2, 13.3, and 15.8 MPa for the corresponding w/c. However, the response was not consistently proportional to fiber dosage: it increased clearly with dosage for CF at w/c = 0.50 and 0.60, but not for RF or for CF at w/c = 0.40, indicating that the peak flexural response was governed by the combined effects of fiber type, dosage, and matrix quality.

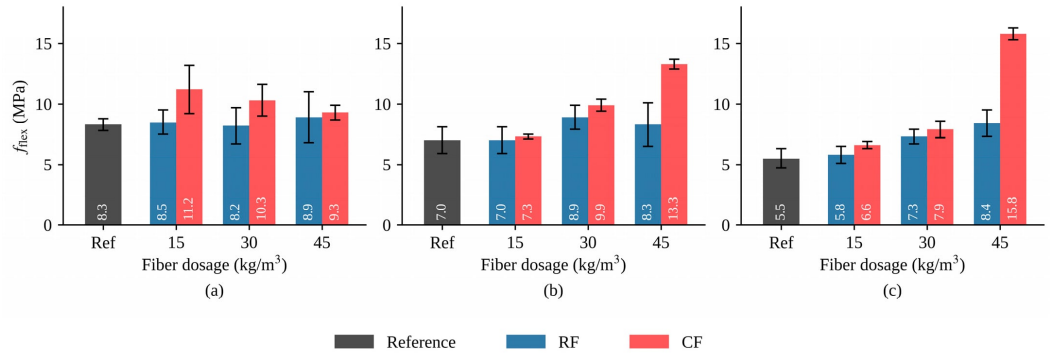


Figure 4. f_{flex} of RF- and CF-reinforced concrete at different fiber dosages: (**a**) w/c = 0.40; (**b**) w/c = 0.50; and (**c**) w/c = 0.60. Error bars represent ± standard deviation.

Three-way ANOVA indicated that f_{flex} was governed mainly by fiber type and dosage ($p < 0.001$), with higher values for CF than for RF, whereas the effect of w/c was not significant ($p > 0.05$); the effect of dosage depended on w/c ($p < 0.001$). Compared with the reference mixtures, f_{flex} increased significantly only at higher fiber dosages and at w/c ≥ 0.50 (Dunnett's test, $p < 0.05$).

Although f_{flex} describes the peak flexural response, it does not fully characterize the contribution of fibers after cracking. Therefore, f_{R1} and f_{R3}, corresponding to CMOD values of 0.5 and 2.5 mm, respectively, were used to characterize the residual response at early and more advanced stages of crack opening. As summarized in Table 4, the distinction between these two stages was particularly evident for RF mixtures. At 45 kg/m^3, f_{R1} values of 4.36, 4.09, and 4.15 MPa decreased to f_{R3} values of 2.52, 2.39, and 2.54 MPa for w/c ratios of 0.40, 0.50, and 0.60, respectively. In contrast, CF maintained or increased its residual capacity at higher dosages; at 45 kg/m^3, f_{R1} and f_{R3} were 7.19 and 5.95 MPa at w/c = 0.40, 11.15 and 12.10 MPa at w/c = 0.50, and 12.52 and 13.13 MPa at w/c = 0.60. Thus, considering both f_{R1} and f_{R3} reveals a clear difference in the evolution of post-cracking behavior: RF provided substantial early residual capacity but generally exhibited greater strength loss with increasing crack opening, whereas CF, particularly at higher dosages, provided a more sustained residual response. Toughness was additionally evaluated to characterize the overall energy absorption capacity, and the complete results are presented in Table 3.

Toughness results further confirmed the contribution of fibers to post-cracking performance. While the reference mixtures exhibited toughness values of only 1362–1593 N.mm, the maximum values reached 14,199–23,425 N.mm for RF and 30,500–39,881 N.mm for CF. CF showed a more consistent increase in toughness with fiber dosage, whereas RF exhibited a more variable response. A three-way ANOVA showed that fiber type, fiber dosage, and w/c ratio all significantly affected toughness ($p < 0.001$), with fiber type and dosage explaining most of the variance. All fiber-reinforced mixtures had higher toughness than the plain concrete, and CF mixtures had higher toughness than RF mixtures at the same w/c ratio and dosage ($p < 0.01$), except at 0.50/15. Notably, 0.50/45RF combined a relatively low f_{R3} of 2.39 MPa with a toughness of 23,425 N.mm. This apparent contradiction arises because f_{R3} reflects the load at a single crack opening (CMOD = 2.5 mm), whereas toughness integrates the load over the entire CMOD range up to 4.0 mm. In this mixture, f_{R1} (4.09 MPa) was considerably higher than f_{R3}, indicating that the load was carried mainly at small and intermediate crack openings and decreased gradually thereafter. This behavior is consistent with the progressive pull-out of the irregular recycled fibers, which was the predominant failure mode observed in the fractured specimens.

Table 4. Residual flexural strength and toughness of SFRC mixtures.

Mix	f_{R1} (MPa)	f_{R3} (MPa)	Toughness (N.mm)
0.40/Ref	—	—	1593 ± 488
0.40/15RF	2.83 ± 0.33	2.14 ± 0.17	11,384 ± 1478
0.40/30RF	4.15 ± 0.48	2.83 ± 0.32	15,179 ± 1668
0.40/45RF	4.36 ± 1.01	2.52 ± 0.57	17,741 ± 1273
0.40/15CF	3.86 ± 0.29	3.10 ± 0.13	15,906 ± 1128
0.40/30CF	5.52 ± 0.37	5.80 ± 0.30	26,206 ± 1328
0.40/45CF	7.19 ± 0.49	5.95 ± 0.48	30,500 ± 1578
0.50/Ref	—	—	1362 ± 354
0.50/15RF	3.16 ± 0.26	3.49 ± 0.32	14,722 ± 1255
0.50/30RF	3.41 ± 0.47	2.48 ± 0.33	12,966 ± 1125
0.50/45RF	4.09 ± 0.68	2.39 ± 0.46	23,425 ± 1529
0.50/15CF	2.68 ± 0.19	2.70 ± 0.11	12,415 ± 947
0.50/30CF	6.58 ± 0.54	6.93 ± 0.54	27,668 ± 1147
0.50/45CF	11.15 ± 0.82	12.10 ± 0.48	34,711 ± 1471
0.60/Ref	—	—	1500 ± 234
0.60/15RF	1.85 ± 0.25	1.34 ± 0.13	7201 ± 1147
0.60/30RF	4.16 ± 0.44	2.94 ± 0.31	13,793 ± 1329
0.60/45RF	4.15 ± 0.79	2.54 ± 0.44	14,199 ± 1322
0.60/15CF	3.08 ± 0.22	3.77 ± 0.26	16,568 ± 617
0.60/30CF	4.36 ± 0.31	4.76 ± 0.42	21,245 ± 981
0.60/45CF	12.52 ± 0.94	13.13 ± 1.08	39,881 ± 1051

3.3. Multi-Criteria Assessment

The responses evaluated in this study did not vary in the same direction with fiber type and dosage. Increasing the fiber dosage reduced workability and did not systematically change compressive strength, whereas residual strength and toughness generally increased. When performance criteria conflict in this way, no single response can identify the most suitable mixture, and multi-criteria optimization provides a mathematical basis for comparing the alternatives [28]. The desirability function approach has been applied to concretes containing steel fibers recovered from scrap tires, where mechanical properties and cost were considered together [28,29]. In the present study, it was applied to compressive strength (d_1), f_{R3} (d_2), and toughness (d_3) with equal importance.

All 18 fiber-reinforced mixtures were included in the analysis, and the minimum and maximum values observed for each response were used for normalization (Equation (1)). The resulting D values therefore represent the relative mechanical performance of the mixtures within the investigated experimental domain. Because D is a geometric mean, it approaches zero when any response is close to its minimum, which penalizes mixtures with unbalanced performance [28,29]. Representative results corresponding to the highest D value for each fiber type at each w/c ratio are presented in Table 5.

Table 5. Representative desirability results for RF and CF mixtures.

Mix	d_1	d_2	d_3	D
0.40/30RF	0.754	0.126	0.244	0.285
0.40/45CF	1.000	0.391	0.713	0.653
0.50/45RF	0.263	0.089	0.496	0.226
0.50/45CF	0.286	0.913	0.842	0.604
0.60/30RF	0.020	0.136	0.202	0.082
0.60/45CF	0.020	1.000	1.000	0.272

The highest overall desirability was obtained for 0.40/45CF ($D = 0.653$), followed by 0.50/45CF ($D = 0.604$). Among the RF mixtures, 0.40/30RF exhibited the highest value ($D = 0.285$), while increasing the RF dosage to 45 kg/m^3 did not further improve the combined mechanical response at this w/c ratio. At each w/c ratio, the best CF mixture reached a higher D than the best RF mixture (Table 5), reflecting the higher residual strength and toughness of CF (Section 3.2). The variation in D over the investigated range is shown in Figure 5. For CF, D increased markedly toward low w/c and high fiber dosage, whereas the RF surface was considerably flatter and reached its maximum at w/c = 0.40 and an intermediate dosage. The results also illustrate the importance of considering multiple responses simultaneously. Although 0.60/45CF achieved the highest f_{R3} (13.13 MPa) and toughness (39,881 N.mm) in the experimental program, its very low compressive-strength desirability ($d_1 = 0.020$) limited the overall index to $D = 0.272$. In contrast, 0.50/45CF, with a higher d_1 of 0.286 and slightly lower d_2 and d_3 (0.913 and 0.842), reached $D = 0.604$. This comparison shows that the geometric mean strongly penalizes a very low individual desirability, so the highest value of an individual response does not ensure the highest overall desirability.

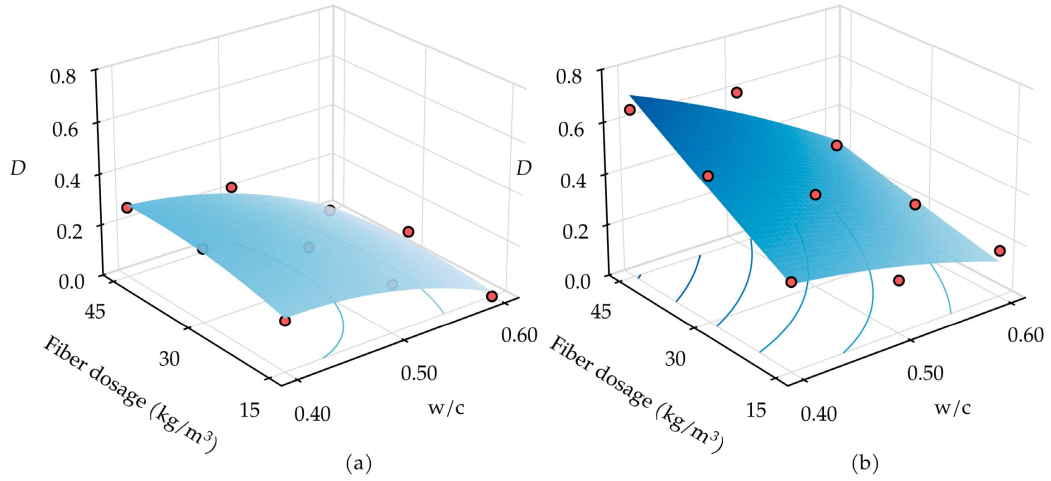


Figure 5. Overall desirability (D) as a function of w/c and fiber dosage: (**a**) RF; (**b**) CF. Markers indicate the calculated D values of the tested mixtures, and the surfaces show second-order polynomial fits. Darker blue indicates higher D.

The fitted equations were (Figure 5):

$$for\ RF: D = -0.838 + 4.321(^{w}/_{c}) + 0.0151F - 0.01317(^{w}/_{c})F - 5.046(^{w}/_{c})^2 - 1.20 \times 10^{-4}F^2 \quad (5)$$

$$for\ CF: D = -0.2475 + 1.928(^{w}/_{c}) + 0.02642F - 0.03694(^{w}/_{c})F - 2.334(^{w}/_{c})^2 + 1.70 \times 10^{-5}F^2 \quad (6)$$

The coefficients of determination were $R^2 = 0.929$ for RF and $R^2 = 0.937$ for CF. With six coefficients fitted to nine points, these surfaces indicate trends within the investigated domain and should not be used as predictive equations.

4. Conclusions

This study compared RF and CF in OPC concrete at three w/c ratios (0.40, 0.50, and 0.60) and fiber dosages of 15, 30, and 45 kg/m^3. Based on the experimental results, the following conclusions can be drawn:

- RF caused a greater reduction in workability than CF, particularly at higher fiber dosages and lower w/c ratios. In contrast, compressive strength was governed mainly by matrix quality, with no systematic improvement observed with increasing fiber dosage.

- Both fiber types improved the flexural and post-cracking response, but CF generally provided higher residual strengths. RF exhibited a greater reduction in residual capacity between fR1 and fR3, whereas CF, particularly at higher dosages, maintained or increased its load-carrying capacity with increasing crack opening.
- Toughness increased substantially with fiber incorporation. The maximum toughness values obtained with RF ranged from 14,199 to 23,425 N.mm across the three w/c ratios, while CF reached 30,500–39,881 N.mm. The CF mixtures also showed a more consistent increase in toughness with increasing fiber dosage.
- The multi-criteria assessment confirmed that overall mechanical performance depended on the combined effects of matrix quality, fiber type, and dosage. The highest overall desirability was obtained for 0.40/45CF (D = 0.653), whereas 0.40/30RF provided the highest desirability among the RF mixtures (D = 0.285). Increasing RF dosage beyond 30 kg/m^3 therefore did not necessarily result in a better combined mechanical response.

Overall, RF can provide meaningful post-cracking capacity and energy absorption, but its response is more sensitive to fiber dosage and matrix quality than that of CF. The results highlight that recycled tire steel fibers should be evaluated based on the required level of post-cracking performance rather than considered as a direct equivalent replacement for manufactured steel fibers.

Author Contributions: Conceptualization, C.C. and O.S.; methodology, C.C. and O.S.; validation, C.C. and O.S.; formal analysis, C.C.; investigation, C.C.; resources, O.S.; data curation, C.C.; writing—original draft preparation, C.C.; writing—review and editing, C.C. and O.S.; visualization, C.C.; supervision, O.S.; project administration, O.S. All authors have read and agreed to the published version of the manuscript.

Funding: This research received no external funding.

Institutional Review Board Statement: Not applicable.

Informed Consent Statement: Not applicable.

Data Availability Statement: The raw data supporting the conclusions of this article will be made available by the authors on request.

Acknowledgments: The authors have reviewed and edited the output and take full responsibility for the content of this publication.

Conflicts of Interest: The authors declare no conflicts of interest.

Abbreviations

The following abbreviations are used in this manuscript:

CF	Commercial steel fiber
CMOD	Crack mouth opening displacement
D	Overall desirability
ELT	End-of-life tire
OPC	Ordinary Portland cement
RF	Recycled tire steel fiber
SFRC	Steel fiber-reinforced concrete
SP	Superplasticizer

References

1. ETRMA. In Europe 95% of All End-of-Life Tyres Were Collected and Treated in 2019. Available online: https://www.etrma.org/wp-content/uploads/2021/05/20210520_ETRMA_PRESS-RELEASE_ELT-2019.pdf (accessed on 2 October 2026).

2. Kolendo, G.; Voronova, V.; Bumanis, G.; Korjakins, A.; Bajare, D. Life Cycle Assessment of End-of-Life Tire Disposal Methods and Potential Integration of Recycled Crumb Rubber in Cement Composites. *Appl. Sci.* **2024**, *14*, 11667. [CrossRef]
3. Backes, J.G.; Del Rosario, P.; Luthin, A.; Traverso, M. Comparative Life Cycle Assessment of End-of-Life Scenarios of Carbon-Reinforced Concrete: A Case Study. *Appl. Sci.* **2022**, *12*, 9255. [CrossRef]
4. Xiao, Z.; Pramanik, A.; Basak, A.K.; Prakash, C.; Shankar, S. Material Recovery and Recycling of Waste Tyres—A Review. *Clean. Mater.* **2022**, *5*, 100115. [CrossRef]
5. Bockstal, L.; Berchem, T.; Schmetz, Q.; Richel, A. Devulcanisation and Reclaiming of Tires and Rubber by Physical and Chemical Processes: A Review. *J. Clean. Prod.* **2019**, *236*, 117574. [CrossRef]
6. Liew, K.M.; Akbar, A. The Recent Progress of Recycled Steel Fiber Reinforced Concrete. *Constr. Build. Mater.* **2020**, *232*, 117232. [CrossRef]
7. Buratti, N.; Mazzotti, C.; Savoia, M. Post-Cracking Behaviour of Steel and Macro-Synthetic Fibre-Reinforced Concretes. *Constr. Build. Mater.* **2011**, *25*, 2713–2722. [CrossRef]
8. Bentur, A.; Mindess, S. *Fibre Reinforced Cementitious Composites*; E & FN Spon: London, UK, 1990.
9. Centonze, G.; Leone, M.; Aiello, M.A. Steel Fibers from Waste Tires as Reinforcement in Concrete: A Mechanical Characterization. *Constr. Build. Mater.* **2012**, *36*, 46–57. [CrossRef]
10. Hu, H.; Papastergiou, P.; Angelakopoulos, H.; Guadagnini, M.; Pilakoutas, K. Mechanical Properties of SFRC Using Blended Manufactured and Recycled Tyre Steel Fibres. *Constr. Build. Mater.* **2018**, *163*, 376–389. [CrossRef]
11. Hu, H.; Papastergiou, P.; Angelakopoulos, H.; Guadagnini, M.; Pilakoutas, K. Mechanical Properties of SFRC Using Blended Recycled Tyre Steel Cords (RTSC) and Recycled Tyre Steel Fibres (RTSF). *Constr. Build. Mater.* **2018**, *187*, 553–564. [CrossRef]
12. Niş, A.; Özyurt, N.; Özturan, T. Variation of Flexural Performance Parameters Depending on Specimen Size and Fiber Properties. *J. Mater. Civ. Eng.* **2020**, *32*, 04020054. [CrossRef]
13. Senesavath, S.; Salem, A.; Kashkash, S.; Zehra, B.; Orban, Z. The Effect of Recycled Tyre Steel Fibers on the Properties of Concrete. *Pollack Period.* **2022**, *17*, 43–49. [CrossRef]
14. Alsaif, A.; Fares, G.; Alhozaimy, A. Effectiveness of Ultra-High-Performance Concrete Containing Recycled Tire Steel Fibers and High-Volume Scoria Rock Powder as Natural Pozzolan. *Case Stud. Constr. Mater.* **2024**, *21*, e03841. [CrossRef]
15. Su, P.; Li, M.; Dai, Q.; Wang, J. Mechanical and Durability Performance of Concrete with Recycled Tire Steel Fibers. *Constr. Build. Mater.* **2023**, *394*, 132287. [CrossRef]
16. Neves, A.; Almeida, J.; Cruz, F.; Miranda, T.; Cunha, V.M.C.F.; Rodrigues, M.; Costa, J.; Pereira, E.B. Design Procedures for Sustainable Structural Concretes Using Wastes and Industrial By-Products. *Appl. Sci.* **2023**, *13*, 2087. [CrossRef]
17. Abdolpour, H.; Muthu, M.; Niewiadomski, P.; Sadowski, Ł.; Hojdys, Ł.; Krajewski, P.; Kwiecień, A. Green Manufacturing of UHPFRC Made with Waste Derived from Scrap Tires and Oil Refineries. *Appl. Sci.* **2024**, *14*, 5313. [CrossRef]
18. Colak, C.; Sengul, O. Residual Flexural Performance and Performance-Normalized Embodied Carbon of Recycled and Commercial Steel Fibers in Slag-Blended Concrete. *J. Compos. Sci.* **2025**, *9*, 656. [CrossRef]
19. Bekaert. *Dramix® 3D 80/60BG Datasheet*; Bekaert: Zwevegem, Belgium, 2019. Available online: https://www.bekaert.com/dramix/downloads (accessed on 23 October 2026).
20. *EN 12390-3:2019*; Testing Hardened Concrete—Part 3: Compressive Strength of Test Specimens. European Committee for Standardization (CEN): Brussels, Belgium, 2019.
21. *EN 14651:2005+A1:2007*; Test Method for Metallic Fibre Concrete—Measuring the Flexural Tensile Strength (Limit of Proportionality (LOP), Residual). European Committee for Standardization (CEN): Brussels, Belgium, 2007.
22. Derringer, G.; Suich, R. Simultaneous Optimization of Several Response Variables. *J. Qual. Technol.* **1980**, *12*, 214–219. [CrossRef]
23. Peng, M.; Gao, Y.; Wei, J.; Han, Y.; Chen, X.; Kou, X. Experimental Study on Mechanical Properties and Toughness of Recycled Steel Fiber Rubber Concrete. *Case Stud. Constr. Mater.* **2024**, *21*, e03858. [CrossRef]
24. Alsaif, A.; Koutas, L.; Bernal, S.A.; Guadagnini, M.; Pilakoutas, K. Mechanical Performance of Steel Fibre Reinforced Rubberised Concrete for Flexible Concrete Pavements. *Constr. Build. Mater.* **2018**, *172*, 533–543. [CrossRef]
25. Alsaif, A.; Alharbi, Y.R. Strength, Durability and Shrinkage Behaviours of Steel Fiber Reinforced Rubberized Concrete. *Constr. Build. Mater.* **2022**, *345*, 128295. [CrossRef]
26. Hassan, A.M.T.; Jones, S.W.; Mahmud, G.H. Experimental Test Methods to Determine the Uniaxial Tensile and Compressive Behaviour of Ultra High Performance Fibre Reinforced Concrete (UHPFRC). *Constr. Build. Mater.* **2012**, *37*, 874–882. [CrossRef]
27. Le Hoang, A.; Fehling, E. Influence of Steel Fiber Content and Aspect Ratio on the Uniaxial Tensile and Compressive Behavior of Ultra High Performance Concrete. *Constr. Build. Mater.* **2017**, *153*, 790–806. [CrossRef]

28. Sengul, O. Mechanical Behavior of Concretes Containing Waste Steel Fibers Recovered from Scrap Tires. *Constr. Build. Mater.* **2016**, *122*, 649–658. [CrossRef]
29. Sengul, O. Mechanical Properties of Slurry Infiltrated Fiber Concrete Produced with Waste Steel Fibers. *Constr. Build. Mater.* **2018**, *186*, 1082–1091. [CrossRef]

Disclaimer/Publisher's Note: The statements, opinions and data contained in all publications are solely those of the individual author(s) and contributor(s) and not of MDPI and/or the editor(s). MDPI and/or the editor(s) disclaim responsibility for any injury to people or property resulting from any ideas, methods, instructions or products referred to in the content.